The interaction between ORF18 and ORF30 is required for late gene expression in Kaposi's sarcoma-associated herpesvirus

Angelica F Castañeda[a], and Britt A Glaunsinger[a,b,#]

[a] Department of Plant & Microbial Biology, University of California Berkeley, CA, USA

[b] Howard Hughes Medical Institute, Berkeley, CA, USA

[#]Corresponding Author: glaunsinger@berkeley.edu

Running title: Late gene expression requires ORF18-ORF30 interaction

Abstract

In the beta- and gammaherpesviruses, a specialized complex of viral transcriptional activators (vTAs) coordinate to direct expression of virus-encoded late genes, which are critical for viral assembly and whose transcription initiates only after the onset of viral DNA replication. The vTAs in Kaposi's sarcoma-associated herpesvirus (KSHV) are ORF18, ORF24, ORF30, ORF31, ORF34, and ORF66. While the general organization of the vTA complex has been mapped, the individual roles of these proteins, and how they coordinate to activate late gene promoters, remains largely unknown. Here, we performed a comprehensive mutational analysis of the conserved residues in ORF18, which is a highly interconnected vTA component. Surprisingly, the mutants were largely selective for disrupting the interaction with ORF30 but not the other three ORF18 binding partners. Furthermore, disrupting the ORF18-ORF30 interaction weakened the vTA complex as a whole, and an ORF18 point mutant that failed to bind ORF30 was unable

22 to complement an ORF18 null virus. Thus, contacts between individual vTAs are critical, as even
23 small disruptions in this complex result in profound defects in KSHV late gene expression.
24
25 **Importance**
26 Kaposi's sarcoma-associated herpesvirus (KSHV) is the etiologic agent of Kaposi's sarcoma and
27 other B-cell cancers and remains a leading cause of death in immunocompromised individuals.
28 A key step in the production of infectious virions is the transcription of viral late genes, which
29 generates capsid and structural proteins and requires the coordination of six viral proteins that
30 form a complex. The role of these proteins during transcription complex formation and the
31 importance of protein-protein interactions are not well understood. Here, we focused on a
32 central component of the complex, ORF18, and revealed that disruption of its interaction with
33 even a single component of the complex (ORF30) prevents late gene expression and completion
34 of the viral lifecycle. These findings underscore how individual interactions between the late
35 gene transcription components are critical for both the stability and function of the complex.
36
37 **Introduction**
38 A broadly conserved feature of the lifecycle of dsDNA viruses is that replication of the
39 viral genome licenses transcription of a specific class of viral transcripts termed late genes.
40 There is an intuitive logic behind this coupling, as late genes encode proteins that participate in
41 progeny virion assembly and egress, and thus are not needed until newly synthesized genomes
42 are ready for packaging. Additionally, late gene transcription requires ongoing DNA replication,
43 and in the gammaherpesviruses Kaposi's sarcoma-associated herpesvirus (KSHV) and Epstein-

44 Barr virus (EBV) the increase in template abundance appears insufficient to explain the robust
45 transcription of late genes whose products are required in large amounts (1).

46 While the mechanisms underlying late gene activation can vary across viral families, in
47 the beta- and gammaherpesviruses, late gene promoters are strikingly minimalistic and
48 primarily consist of a modified TATA box (TATT) and ~10-15 base pairs of variable flanking
49 sequence (2–5). Despite this sequence simplicity, their transcription requires a dedicated set of
50 at least six conserved viral transcriptional activators (vTAs) whose precise roles are only
51 beginning to be uncovered. In KSHV, the vTAs are encoded by open reading frames (ORFs) 18,
52 24, 30, 31, 34, and 66 (6–15). The best characterized of the vTAs is a viral TATA-binding protein
53 (TBP) mimic, encoded by ORF24 in KSHV, which binds both the late gene promoter and RNA
54 polymerase II (Pol II) (4, 8, 16, 17). Beyond the viral TBP mimic, the only other vTA with a
55 documented transcription-related function is pUL79 (homologous to KSHV ORF18) in human
56 cytomegalovirus (HCMV), which promotes transcription elongation at late times of infection
57 (18). Roles for the remaining vTAs remain largely elusive, although the KSHV ORF34 protein and
58 its murine cytomegalovirus (MCMV) homolog pM95 may function as hub proteins, as they
59 interact with numerous other vTAs (7, 9, 19). In addition to the six conserved vTAs, in EBV, the
60 kinase activity of BGLF4 (homologous to KSHV ORF36) also contributes to the expression of late
61 genes (20, 21).

62 Studies in both beta-and gammaherpesviruses indicate that the vTAs form a complex,
63 the general organization of which has been mapped in MCMV and KSHV (7, 9, 10, 19) (Figure
64 1A). Notably, several recent reports demonstrate that specific interactions between the vTAs
65 are critical for late gene transcription. In MCMV, mutation of conserved residues in pM91

66 (homologous to KSHV ORF30) that disrupt its interaction with pM79 (homologous to KSHV
67 ORF18) renders the virus unable to transcribe late genes (19). Similarly, the interaction
68 between KSHV ORFs 24 and 34 can be abrogated by a single amino acid mutation in ORF24
69 which prevents late gene transcription (9). Further delineating these contacts should provide
70 foundational information relevant to understanding vTA complex function.

71 The precise role of KSHV ORF18 in late gene transcription remains unknown, however it
72 is predicted to interact with four of the five other vTAs (ORFs 30, 31, 34, and 66), suggesting
73 that—like ORF34—it may play a central role in vTA complex organization (7, 9). Here, we
74 performed an interaction screen of ORF18 mutants to comprehensively evaluate the roles of its
75 conserved residues in mediating pairwise vTA binding. We reveal that ORF30 is particularly
76 sensitive to mutation in ORF18, enabling isolation of mutants that selectively abrogate this
77 interaction while retaining the contacts between ORF18 and the other vTAs. Disrupting the
78 ORF18-ORF30 interaction not only prevents KSHV late gene transcription as measured by K8.1
79 expression, but also appears to weaken assembly of the remaining vTA complex. These findings
80 underscore the key role that ORF18 plays in late gene transcription and suggest that disrupting
81 just one of its interactions has a destabilizing effect on the vTA complex as a whole.

82

83 **Results**

84 **ORF18 interacts with ORF30, ORF31, ORF34, and ORF66**

85 Previous work using a split luciferase-based interaction screen suggested that ORF18 is
86 highly interconnected with other viral late gene activators, as it interacted with the majority of
87 the proteins in the viral transcription pre-initiation complex (vPIC) (9). To independently

88 confirm the binding of ORF18 to ORFs 30, 31, 34, and 66 in the absence of other viral factors,
89 we assessed its ability to co-immunoprecipitate (co-IP) with each of these vTAs in transfected
90 HEK293T cells. Consistent with the screening data, ORF18-3xFLAG interacted robustly with C-
91 terminal 2xStrep-tagged versions of ORF30, ORF31, and ORF66 (Figure 1B, C, D). Although
92 ORF18-3xFLAG did not interact with ORF34 tagged on its C-terminus, the interaction was
93 recovered upon moving the 2xStrep tag to the N-terminus of ORF34 (Figure 1E). Furthermore,
94 we consistently observed that the expression of ORF30 was higher when co-expressed with
95 ORF18 than when transfected with vector control, suggesting that ORF18 may stabilize ORF30
96 (Figure 1B). To determine whether ORF18 had a stabilizing effect on ORF30, the half-life of
97 ORF30 was measured in both the presence and absence of ORF18. As can be seen in Figure 1F,
98 ORF30 stability increased significantly upon co-expression with ORF18.
99

100 **An interaction screen of ORF18 mutants reveals the role of conserved residues in interactions**
101 **with the other vTAs**

102 To evaluate the importance of the interaction between ORF18 and its individual vTA
103 contacts, we aimed to identify point mutations that disrupted binding to individual vTAs but did
104 not destroy the integrity of the complex. Since the late gene vTA complex is conserved across
105 the beta- and gammaherpesviruses we reasoned that the individual points of contact might
106 depend on conserved amino acid residues. We performed a multiple sequence alignment
107 between KSHV ORF18 and its homologs in five other beta- and gamma herpesviruses (MHV68
108 ORF18, HCMV pUL79, MCMV pM79, EBV BVLF1, and BHV ORF18) using MUSCLE (22). The
109 sequence alignment revealed 25 single conserved residues, including six pairs of adjacent

110 conserved residues, which are depicted in Figure 2A as a schematic of the primary structure of
111 ORF18 showing the positions of conserved residues. We mutated each of the 25 conserved
112 residues to alanine in ORF18-3xFLAG and made double alanine mutations in the six cases of
113 adjacent conserved residues (Figure 2A). Each of these 31 mutants was screened individually
114 for the ability to interact with ORFs 30, 31, and 66 by co-IP followed by western blot (data not
115 shown). To account for differences in expression between the ORF18 mutants, we calculated
116 the co-IP efficiency of each of the mutants, as described in the methods. These data were used
117 to generate a heat map, which displays the pair-wise interaction efficiencies on a color scale
118 where lighter blocks represent reduced binding and darker blocks represents increased binding
119 relative to WT (Figure 2B). Overall, the data revealed that ORF30 was the most sensitive to
120 mutations in ORF18, as 24 out of the 31 mutants displayed reduced or no binding. ORF31
121 showed variable sensitivity to ORF18 mutation (with some mutants even increasing the
122 interaction efficiency), while the ORF66-ORF18 interaction was relatively refractory to the
123 ORF18 point mutations (Figure 2B).

124 We focused on the six ORF18 mutants that exhibited <10% co-IP efficiency, relative to
125 WT, with any vTA in our initial screen (L29A, E36A, L151A, W170A, E36A_L37A, and
126 W170A_G171A; highlighted in red in Figure 2A). These were re-screened 3-4 independent times
127 in co-IP assays with vTA components ORFs 30, 31, 34, and 66, and the co-IP efficiencies were
128 calculated as described in the methods then plotted relative to values obtained for WT ORF18
129 (Figure 3A-D). All six of these ORF18 mutants had severe defects in their ability to co-IP ORF30,
130 but none were consistently different than WT ORF18 for interaction with ORFs 31, 34, and 66
131 (Figure 3B-D). Among the six mutants, $ORF18^{E36A_L37A}$ and $ORF18^{W170A_G171A}$ showed no

132 detectable binding to ORF30, with ORF18^{E36A_L37A} retaining near-WT levels of interaction with
133 the remaining vTAs.
134
135 **ORF18 point mutants that weaken the interaction between ORF18 and ORF30 have a reduced**
136 **capacity to activate the K8.1 late gene promoter**
137 A reporter assay has been developed in which the co-expression of the six individual
138 vTAs can specifically activate a KSHV (or EBV) late gene promoter in transfected HEK293T cells
139 (9, 10). We used this assay as an initial proxy for the ability of the six ORF18 mutants described
140 above to activate late gene transcription. HEK293T cells were co-transfected with each of the
141 vTAs, including either WT or mutant ORF18, and firefly luciferase reporter plasmids driven by
142 either the late K8.1 promoter or, as a control, the early ORF57 promoter (Figure 4A). A plasmid
143 containing constitutively expressed Renilla luciferase was co-transfected with each sample to
144 normalize for transfection efficiency. As expected, inclusion of WT ORF18 with the remaining
145 vTA complex resulted in specific activation of the K8.1 late promoter, but not of the early
146 ORF57 promoter (Figure 4B). ORF18 mutants L29A, E36A, and L151A modestly reduced
147 activation of the late promoter, whereas more significant defects were observed with mutants
148 W170A, E36A_L37A, and W170A_G171A (Figure 4B). Although ORF18^{W170A_G171A} had the most
149 pronounced transcriptional defect, this mutant showed somewhat more variability than
150 ORF18^{E36A_L37A} in its interactions with the other vTA components (Figures 3 & 4). Thus, we
151 considered ORF18^{E36A_L37A} to be the top candidate for selectively analyzing the importance of
152 the ORF18-ORF30 interaction for KSHV late gene transcription.
153

154 **The interaction between ORF18 and ORF30 affects assembly of the vTA complex**

155 The transcriptional defect of the ORF18^{E36A_L37A} mutant in the reporter assay could be
156 due to a defect in assembly of the complex or due to defects in downstream events. To
157 distinguish between these possibilities, WT or mutant ORF18-3xFLAG was co-transfected into
158 HEK293T cells with each of the other Strep-tagged vTAs. We then performed an α-FLAG IP,
159 revealing that purification of WT ORF18 led to co-IP of the complete vTA complex including Pol
160 II, which has been shown to interact with ORF24 in KSHV (8) (Figure 5). We noted that in this
161 assay ORF18^{E36A_L37A} was more weakly expressed than WT ORF18, so to compare complex
162 formation with equivalent amounts of each protein, we titrated down the amount of WT ORF18
163 to match the levels of ORF18^{E36A_L37A}. Similar to our observation in a pairwise co-IP (Figure 1B),
164 the ORF30 protein abundance decreased as the expression of ORF18 was reduced (Figure 5);
165 however, the complete vTA complex still co-purified even with reduced levels of WT ORF18
166 (Figure 5). Notably, the vTA complex was recovered at lower levels in the presence of
167 ORF18^{E36A_L37A}. When imaged at a longer exposure, all of the vTAs, with the exception of ORF30,
168 remained associated with ORF18^{E36A_L37A} (Figure 5, far right panel). Thus, the selective loss of
169 the ORF18-ORF30 interaction may reduce the overall stability of the vTA complex.

170

171 **The interaction between ORF18 and ORF30 is crucial for expression of the late gene K8.1**

172 Next, to characterize the effect of ORF18^{E36A_L37A} on the viral replication cycle, we tested
173 the ability of this mutant to complement the late gene expression defect of a KSHV mutant
174 lacking ORF18 (18.stop) (6). The renal carcinoma cell line iSLK harbors the virus (either WT or
175 18.stop) in a latent state, which can be reactivated upon expression of the doxycycline-

176 inducible major lytic transactivator RTA and treatment with sodium butyrate. Using lentiviral
177 transduction, we generated stable, doxycycline-inducible versions of the 18.stop iSLK cells
178 expressing either ORF18-3xFLAG or ORF18^{E36A_L37A}-3xFLAG (18.stop.ORF18^{WT} and
179 18.stop.ORF18^{E36A_L37A}, respectively). The cells were assayed 72 hours post lytic reactivation for
180 their ability to replicate DNA, express early and late proteins, and produce progeny virions.
181 Although we observed a modest decrease of viral DNA replication in the 18.stop cells, as
182 measured by qPCR, upon complementation with either WT ORF18 or ORF18^{E36A_L37A}, the levels
183 of DNA replication were not significantly different from iSLK cells infected with WT KSHV (Figure
184 6A). Notably, the 18.stop.ORF18^{E36A_L37A} cell line expressed more ORF18 than the
185 18.stop.ORF18^{WT} cell line, in contrast to the reduced expression of the mutant in HEK293T cells
186 (Figure 6B, compare to levels in Figure 5). However, while both reactivated 18.stop.ORF18^{WT}
187 and 18.stop.ORF18^{E36A_L37A} cell lines expressed equivalent levels of the ORF59 early protein,
188 only 18.stop.ORF18^{WT} was able to rescue expression of the model late gene K8.1 (Figure 6B).
189 We then evaluated the level of KSHV virion production from the parental WT KSHV-
190 infected iSLK cells, as well as from the 18.stop, 18.stop.ORF18^{WT}, and 18.stop.ORF18^{E36A_L37A} cell
191 lines using a supernatant transfer assay. KSHV produced from iSLK cells contains a constitutively
192 expressed GFP, enabling quantitation of infected recipient cells by flow cytometry (23).
193 Consistent with its late gene expression defect, neither the 18.stop nor the
194 18.stop.ORF18^{E36A_L37A} cell lines were able to produce progeny virions, whereas virion
195 production in the 18.stop.ORF18^{WT} cells was indistinguishable from the WT KSHV-infected iSLK
196 cells (Figure 6C). Collectively, these data demonstrate that the specific interaction between

197 ORF18 and ORF30 is essential for K8.1 late gene expression and virion production during KSHV
198 infection.
199
200 **The analogous mutation in HCMV pUL79 disrupts its interaction with pUL91**
201 As shown in Figure 7A, the E36_L37 residues are conserved across the beta- and
202 gammaherpesvirus ORF18 homologs. To determine whether these amino acids are similarly
203 important in a betaherpesvirus, we engineered the corresponding double mutation in HCMV
204 pUL79 (pUL79^{E48A_L49A}-3xFLAG). Similar to our observation with KSHV ORF30, HCMV pUL91
205 protein expression was significantly decreased in the absence of its WT pUL79 binding partner
206 (Figure 7B). This is consistent with the idea that pUL79 binding stabilizes pUL91. Furthermore,
207 in co-IP assays we detected a robust interaction between pUL79 and pUL91, which was
208 impaired in the presence of pUL79^{E48A_L49A}, even when we accounted for the expression level
209 differences of pUL91 (Figure 7B). This suggests that the overall protein-protein interface may be
210 conserved in the analogous ORF18-ORF30 interaction across the beta- and
211 gammaherpesviruses.
212
213 **Discussion**
214 Elucidating the architecture of the six-member vPIC complex is central to understanding
215 the mechanism underlying viral late gene expression in beta- and gammaherpesviruses.
216 Although their functions are largely unknown, each of these viral transcription regulators is
217 essential for late gene promoter activation and evidence increasingly suggests that their ability
218 to form a complex is crucial for transcriptional activity (9, 10, 19). Here, we reveal that selective

219 disruption of an individual protein-protein contact between KSHV ORF18 and ORF30 within the
220 vPIC is sufficient to abrogate K8.1 late gene expression and virion production in infected cells,
221 emphasizing the sensitivity of the complex to organizational perturbation.

222 We selected ORF18 for mutational screening due to its ability to form pairwise
223 interactions with the majority of other vPIC components, which suggested that it might serve as
224 an organizational hub for vPIC assembly, similar to what has been proposed for ORF34 (7, 9).
225 However, the 31 tested mutants of ORF18 revealed that conserved residues across the length
226 of the protein are extensively—and largely selectively— required for ORF30 binding. This is in
227 contrast to the interaction between the vPIC components ORF24 and ORF34, where the
228 interaction can be localized to a 17 amino acid stretch of ORF24 (9). The observation that the
229 majority of the ORF18 point mutations that disrupt the interaction with ORF30 do not affect its
230 binding to ORFs 31, 34, and 66 indicates that these mutations do not significantly alter the
231 overall folding or structure of ORF18. In MCMV, the organization of the vTA complex is similar
232 to KSHV, except that pM92 (homologous to KSHV ORF31) interacts with pM87 (homologous to
233 KSHV ORF24), whereas in KSHV this interaction is bridged through ORF34 (19). Our data
234 complement recent findings in MCMV, in which mutations of the ORF30 homolog (pM91) that
235 perturb the interaction with the ORF18 homolog (pM79) similarly cause a defect in the
236 expression of late genes (19). Thus, mutations that disrupt the ORF18-ORF30 protein-protein
237 interface in either protein cause the same phenotype.

238 The ORF18-ORF30 interaction appears sensitive to single amino acid changes in the
239 protein-protein interface. The ORF18^{E36A_L37A} mutation does not impair binding to its other vPIC
240 partners in pairwise co-IP experiments and ORF30 does not engage in pairwise interactions with

241 vPIC components other than ORF18 (7, 9). It is therefore notable that the efficiency of the vPIC
242 complex assembly is reduced in HEK293T cells in the presence of the ORF18^{E36A_L37A} mutant,
243 suggesting that the ORF18-ORF30 interaction contributes to the stability of the complex as a
244 whole. The interaction between ORF18 and ORF30 may change the conformation of ORF18,
245 allowing it to interact more strongly with the other vTAs. Alternatively, the E36A_L37A
246 mutation may contribute to binding defects between ORF18 and the other vTAs that are not
247 observed with pairwise interactions, but are enhanced in the presence of all the ORF18 binding
248 partners.

249 We observed that ORF30 protein expression was consistently higher in the presence of
250 WT ORF18 or ORF18 mutants that retained ORF30 binding, suggesting that ORF18 helps
251 stabilize ORF30. *In silico* protein stability prediction studies have suggested that protein stability
252 is in part affected by protein length, where proteins that are less than 100 amino acids tend to
253 be less stable (24, 25). One explanation for the higher expression of ORF30 in the presence of
254 ORF18 could therefore be that the 77 amino acid ORF30 is protected from degradation by
255 ORF18. Another possibility is that ORF18 helps keep ORF30 correctly folded—this has been
256 proposed as a mechanism that stabilizes proteins which have interaction partners (26). The
257 interaction-induced stability of a protein often correlates with the relative concentration of its
258 binding partners (26), as we observed when we titrated down the amount of ORF18 in the
259 context of the complete vTA complex. A similar observation has been made between KSHV
260 proteins ORF36 and ORF45, where ORF36 was dependent on the interaction with ORF45 for
261 stabilization (27). We did not observe a similar correlation with levels of the other ORF18-
262 associated vPIC proteins, and thus their stability may not require protective interactions. We

263 also observed a stabilizing effect of pUL79 on pUL91, indicating this may be a conserved feature
264 of this interaction in other beta- and gammaherpesviruses.

265 The fact that the late gene expression defect of the ORF18^{E36A_L37A} mutant is
266 exacerbated in the context of the virus, compared to in the plasmid promoter activation assay,
267 likely reflects the fact that the plasmid assay measures basal promoter activation but misses
268 other regulatory components of this cascade. For example, the origin of lytic replication is
269 required *in cis* for late gene expression in related gammaherpesviruses (3, 28) and the reporter
270 assay does not capture the important contribution of viral DNA replication towards late gene
271 expression. This may explain why some mutants that are defective for ORF30 binding (e.g.
272 L29A, E36A, L151A) retain partial plasmid promoter activity; perhaps some weak binding
273 between ORF18 and ORF30 enables basal activation of the promoter in a context where the
274 vPIC components are overexpressed. Alternatively, some of the mutations may cause ORF18 to
275 bind to ORF30 more transiently, but their vPIC interaction becomes stabilized in the presence of
276 a late gene promoter.

277 In summary, the absence of K8.1 late gene expression in the KSHV ORF18.stop-infected
278 cells complemented with ORF18^{E36A_L37A} may derive from a cascade of phenotypes: the failure
279 to recruit ORF30 to the vPIC, the ensuing reduction in the efficiency of overall vPIC complex
280 assembly, and the reduced stability of ORF30 (if it also has additional vPIC-independent
281 functions). Ultimately, generating antibodies that recognize the endogenous KSHV vPIC
282 components will enable these phenotypes to be explored further during infection. In addition,
283 information about the 3-dimensional structure of the vPIC would significantly enhance our

284 understanding of this unique transcription complex, as it is becoming increasingly clear that
285 even small disruptions to the complex dramatically impact completion of the viral lifecycle.
286

287 **Materials and Methods**

288 **Plasmids and Plasmid construction**

289 To generate ORF18-3xFLAG pCDNA4, ORF18 was subcloned into the BamHI and NotI sites of
290 pCDNA-3xFLAG. The point mutations in ORF18 were generated using two primer site-directed
291 mutagenesis with Kapa HiFi polymerase (Roche) with primers 1-62 listed in Table 1. All
292 subsequent plasmids described below were generated using InFusion cloning (Clontech) unless
293 indicated otherwise. To generate plasmid pLVX-TetOneZeo, zeocin resistance was PCR amplified
294 out of plasmid pLJM1-EGFP-Zeo with primers 63/64 (Table 1) and used to replace the
295 puromycin resistance in pLVX-TetOne^{TM}-Puro (Clontech) using the AvrII and MluI restriction
296 sites. To generate pLVX-TetOneZeo-ORF18^{WT}-3xFLAG and pLVX-TetOneZeo-ORF18^{E36A_L37A}-
297 3xFLAG, ORF18^{WT}-3xFLAG and ORF18^{E36_37A}-3xFLAG were PCR amplified from each respective
298 pCDNA4 plasmid using primers 71/72 and inserted into the EcoRI and BamHI sites of pLVX-
299 TetOne-Zeo. To generate UL79-3xFLAG pCDNA4 and UL91-2xStrep pCDNA4, UL79 was PCR
300 amplified with primers 67/68 (Table 1) and UL91 was PCR amplified with primers 69/70 (Table
301 1) from HCMV Towne strain, which was kindly provided by Dr. Laurent Coscoy, and cloned into
302 the BamHI and NotI sites of 3xFLAG (Cterm) pCDNA4 or 2xStrep (Cterm) pCDNA4. UL79^{E48A_L49A}
303 was generated with two primer site-directed mutagenesis using Kapa HiFi polymerase with
304 primers 73/74 (Table 1). To make 2xStrep-ORF34 pCDNA4, ORF34 was PCR amplified from
305 ORF34-2xStrep pCDNA4 with primers 65/66 and cloned into the NotI and XbaI sites of 2xStrep

306 (Nterm) pCDNA4. Plasmid K8.1 Pr pGL4.16 contains the minimal K8.1 promoter and ORF57 Pr
307 pGL4.16 contains a minimal ORF57 early gene promoter and have been described previously
308 (9). Plasmids ORF18-2xStrep pCDNA4, ORF24-2xStrep pCDNA4, ORF30-2xStrep pCDNA4, ORF31-
309 2xStrep pCDNA4, ORF34-2xStrep pCDNA4, and ORF66-2xStrep pCDNA4 have been previously
310 described (8). Plasmid pRL-TK (Promega) was kindly provided by Dr. Russel Vance. Lentiviral
311 packaging plasmids psPAX2 (Addgene plasmid # 12260) and pMD2.G (Addgene plasmid #
312 12259) were gifts from Dr. Didier Trono.
313
314 **Cells and transfections**
315 HEK293T cells (ATCC CRL-3216) were maintained in DMEM supplemented with 10% FBS
316 (Seradygm). The iSLK renal carcinoma cell line harboring the KSHV genome on the bacterial
317 artificial chromosome BAC16 and a doxycycline-inducible copy of the KSHV lytic transactivator
318 RTA (iSLK-BAC16) has been described previously (23). iSLK-BAC16-ORF18.stop cells that contain
319 a stop mutation in ORF18 were kindly provided by Dr. Ting-Ting Wu (6). iSLK-BAC16 and iSLK-
320 BAC16-ORF18.stop were maintained in DMEM supplemented with 10% FBS, 1 mg/ml
321 hygromycin, and 1 μg/ml puromycin (iSLK-BAC16 media). iSLK-BAC16-ORF18.stop cells were
322 complemented by lentiviral transduction with ORF18^{WT}-3xFLAG or ORF18^{E36A_L37A}-3xFLAG. To
323 generate the lentivirus, HEK293T cells were co-transfected with pLVX-TetOneZeo-ORF18^{WT}-
324 3xFLAG or pLVX-TetOneZeo-ORF18^{E36A_L37A}-3xFLAG along with the packaging plasmids pMD2.G
325 and psPAX2. After 48h, the supernatant was harvested and syringe-filtered through a 0.45 μm
326 filter (Millipore). The supernatant was diluted 1:2 with DMEM and polybrene was added to a
327 final concentration of 8 μg/ml. 1 x 10^6 iSLK-BAC16-ORF18.stop freshly trypsinized cells were

328 spinfected in a 6-well plate for 2 h at 500 x *g*. After 24 h the cells were expanded to a 10 cm
329 tissue culture plate and selected for 2 weeks in iSLK-BAC16 media supplemented with 325
330 μg/ml zeocin (Sigma). For DNA transfections, HEK293T cells were plated and transfected after
331 24 h at 70% confluency with PolyJet (SignaGen).
332
333 **Immunoprecipitation and western blotting**
334 Cell lysates were prepared 24 h after transfection by washing and pelleting cells in cold
335 PBS, then resuspending the pellets in IP lysis buffer [50 mM Tris-HCl pH 7.4, 150 mM NaCl, 1mM
336 EDTA, 0.5% NP-40, and protease inhibitor (Roche)] and rotating for 30 minutes at 4 °C. Lysates
337 were cleared by centrifugation at 21,000 x *g* for 10 min, then 1 mg (for pairwise interaction IPs)
338 or 2 mg (for the entire late gene complex IPs) of lysate was incubated with pre-washed M2 anti-
339 FLAG magnetic beads (Sigma) overnight. The beads were washed 3x for 5 min each with IP
340 wash buffer [50 mM Tris-HCl pH 7.4, 150 mM NaCl, 1mM EDTA, 0.05% NP-40] and eluted with
341 2x Laemmli sample buffer (BioRad).
342 Lysates and elutions were resolved by SDS-PAGE and western blotted in TBST (Tris-
343 buffered saline, 0.2% Tween 20) using the following primary antibodies: Strep-HRP (Millipore,
344 1:2500); rabbit anti-FLAG (Sigma, 1:3000); mouse anti-FLAG (Sigma, 1:1000); rabbit anti-
345 Vinculin (Abcam, 1:1000); mouse anti-GAPDH (Abcam, 1:1000); mouse anti-Pol II CTD clone
346 8WG16 (Abcam, 1:1000); rabbit anti-K8.1 (1:10000); rabbit anti-ORF59 (1:10000). Rabbit anti-
347 ORF59 and anti-K8.1 was produced by the Pocono Rabbit Farm and Laboratory by immunizing
348 rabbits against MBP-ORF59 or MBP-K8.1 [gifts from Denise Whitby (29)]. Following incubation
349 with primary antibodies, the membranes were washed with TBST and incubated with the

350 appropriate secondary antibody. The secondary antibodies used were the following: goat anti-
351 mouse-HRP (1:5000, Southern Biotech) and goat anti-rabbit-HRP (1:5000, Southern Biotech).
352 The co-IP efficiency for the pairwise interactions was quantified from the western blot
353 images using Image Lab software (BioRad). The band intensity for the both the Strep-tagged
354 ORF and ORF18^{WT}-3xFLAG or ORF18^{Mu}-3xFLAG was calculated for the IP lanes of the western
355 blot. The ratio of the band intensity of Strep-tagged ORF to ORF18^{Mu}-3xFLAG was divided by the
356 ratio of Strep-tagged ORF to ORF18^{WT}-3xFLAG to generate a co-IP efficiency for each ORF18^{Mu}
357 relative to the co-IP efficiency of ORF18^{WT}.
358
359 **ORF30 Protein Stability**
360 Translation was inhibited 24 h after transfection by the addition of 100 μg/ml
361 cycloheximide for 0-8h. Cells were washed once in cold PBS, and cell pellets were frozen until
362 all samples were collected. The pellets were lysed in IP lysis buffer by rotating for 30 minutes at
363 4 °C. Lysates were cleared by centrifugation at 21,000 x *g* for 10 min, then resolved by SDS-
364 PAGE followed by western blot.
365
366 **Virus Characterization**
367 For reactivation studies, 1 x 10^6 iSLK cells were plated in 10 cm dishes for 16 h, then
368 induced with 1 μg/ml doxycycline and 1 mM sodium butyrate for an additional 72 h. To
369 determine the fold DNA induction in reactivated cells, the cells were scraped and triturated in
370 the induced media, and 200 μl of the cell/supernatant suspension was treated overnight with
371 80 μg/ml proteinase K (Promega) in 1x proteinase K digestion buffer (10 mM Tris-HCl pH 7.4,

372 100 mM NaCl, 1 mM EDTA, 0.5% SDS) after which DNA was extracted using a Quick-DNA
373 Miniprep kit (Zymo). Viral DNA fold induction was quantified by qPCR using iTaq Universal SYBR
374 Green Supermix (BioRad) on a QuantStudio3 Real-Time PCR machine with primers 75/76 (Table
375 1) for the KSHV ORF59 promoter and normalized to the level of GAPDH promoter with primers
376 77/78 (Table 1).

377 Infectious virion production was determined by supernatant transfer assay. Supernatant
378 from induced iSLK cells was syringe-filtered through a 0.45 μm filter and diluted 1:2 with
379 DMEM, then 2 mL of the supernatant was spinoculated onto 1 x 10^6 freshly trypsinized
380 HEK293T cells for 2 h at 500 x *g*. After 24 h, the media was aspirated, the cells were washed
381 once with cold PBS and crosslinked in 4% PFA (Ted Pella) diluted in PBS. The cells were pelleted,
382 resuspended in PBS, and a minimum of 50,000 cells/sample were analyzed on a BD Accuri 6
383 flow cytometer. The data were analyzed using FlowJo (30).

384

385 **Late Gene Reporter Assay**

386 HEK293T cells were plated in 6-well plate and each well was transfected with 900 ng of DNA
387 containing 125 ng each of pcDNA4 ORF18-3xFLAG or ORF18^{Mu}-3xFLAG, ORF24-2xStrep, ORF30-
388 2xStrep, ORF31-2xStrep, 2xStrep-ORF34, ORF66-2xStrep, and either K8.1 Pr pGL4.16 or ORF57
389 Pr pGL4.16, along with 25 ng of pRL-TK as an internal transfection control. After 24 h, the cells
390 were rinsed once with PBS, lysed by rocking for 15 min at room temperature in 500 μl of
391 Passive Lysis Buffer (Promega), and clarified by centrifuging at 21,000 x *g* for 2 min. 20 μl of the
392 clarified lysate was added in triplicate to a white chimney well microplate (Greiner bio-one) to
393 measure luminescence on a Tecan M1000 microplate reader using a Dual Luciferase Assay Kit

394 (Promega). The firefly luminescence was normalized to the internal Renilla luciferase control for
395 each transfection.
396
397 **Acknowledgements**
398 We thank all members of the Glaunsinger and Coscoy labs, in particular Matthew R
399 Gardner, for their helpful suggestions and critical reading of the manuscript. This material is
400 based upon work supported by the National Science Foundation Graduate Research Fellowship
401 under Grant No. DGE 1752814 and UC Berkeley Chancellor's Fellowship awarded to A.C. B.G. is
402 an investigator of the Howard Hughes Medical Institute. This research was also supported by
403 NIH R01AI122528 to B.G.
404
405 **References**
406 1. Li D, Fu W, Swaminathan S. 2018. Continuous DNA replication is required for late gene
407 transcription and maintenance of replication compartments in gammaherpesviruses.
408 PLoS Pathog 14:1–25.
409 2. Serio TR, Cahill N, Prout ME, Miller G. 1998. A functionally distinct TATA box required for
410 late progression through the Epstein-Barr virus life cycle. J Virol 72:8338–8343.
411 3. Tang S, Yamanegi K, Zheng Z-M. 2004. Requirement of a 12-base-pair TATT-containing
412 sequence and viral lytic DNA replication in activation of the Kaposi's sarcoma-associated
413 herpesvirus K8.1 late promoter. J Virol 78:2609–2614.
414 4. Wong-Ho E, Wu TT, Davis ZH, Zhang BQ, Huang J, Gong H, Deng HY, Liu FY, Glaunsinger B,
415 Sun R. 2014. Unconventional Sequence Requirement for Viral Late Gene Core Promoters

416 of Murine Gammaherpesvirus 68. J Virol 88:3411–3422.

417 5. Djavadian R, Hayes M, Johannsen E. 2018. CAGE-seq analysis of Epstein-Barr virus lytic
418 gene transcription: 3 kinetic classes from 2 mechanisms. PLoS Pathog 14:1–26.

419 6. Gong D, Wu NC, Xie Y, Feng J, Tong L, Brulois KF, Luan H, Du Y, Jung JU, Wang C -y., Kang
420 MK, Park N-H, Sun R, Wu T-T. 2014. Kaposi's Sarcoma-Associated Herpesvirus ORF18 and
421 ORF30 Are Essential for Late Gene Expression during Lytic Replication. J Virol 88:11369–
422 11382.

423 7. Nishimura M, Watanabe T, Yagi S, Yamanaka T, Fujimuro M. 2017. Kaposi's sarcoma-
424 associated herpesvirus ORF34 is essential for late gene expression and virus production.
425 Sci Rep 7:1–12.

426 8. Davis ZH, Verschueren E, Jang GM, Kleffman K, Johnson JR, Park J, Shales M, Dollen J Von,
427 Maher MC, Johnson T, Newton W, Ja S, Horner J, Hernandez RD, Krogan NJ, Glaunsinger
428 B a. 2015. Global Mapping of Herpesvirus-Host Protein Complexes Reveals a
429 Transcription Strategy for Late Genes. Mol Cell 57:349–360.

430 9. Davis ZH, Hesser CR, Park J, Glaunsinger A. 2016. Associated Herpesvirus Late Gene
431 Transcription Factor Complex Is Essential for Viral Late Gene Expression. J Virol 90:599–
432 604.

433 10. Aubry V, Mure F, Mariame B, Deschamps T, Wyrwicz LS, Manet E, Gruffat H. 2014.
434 Epstein-Barr Virus Late Gene Transcription Depends on the Assembly of a Virus-Specific
435 Preinitiation Complex. J Virol 88:12825–12838.

436 11. Wu T-T, Park T, Kim H, Tran T, Tong L, Martinez-Guzman D, Reyes N, Deng H, Sun R. 2009.
437 ORF30 and ORF34 are essential for expression of late genes in murine gammaherpesvirus

438 68. J Virol 83:2265–2273.

439 12. Arumugaswami V, Wu T-T, Martinez-Guzman D, Jia Q, Deng H, Reyes N, Sun R. 2006.
440 ORF18 is a transfactor that is essential for late gene transcription of a gammaherpesvirus.
441 J Virol 80:9730–9740.

442 13. Jia Q, Wu T-T, Liao H-I, Chernishof V, Sun R. 2004. Murine gammaherpesvirus 68 open
443 reading frame 31 is required for viral replication. J Virol 78:6610–6620.

444 14. Brulois K, Wong L-Y, Lee H-R, Sivadas P, Ensser A, Feng P, Gao S-J, Toth Z, Jung JU. 2015.
445 Association of Kaposi's Sarcoma-Associated Herpesvirus ORF31 with ORF34 and ORF24 Is
446 Critical for Late Gene Expression. J Virol 89:6148–54.

447 15. Wong E, Wu T-T, Reyes N, Deng H, Sun R. 2007. Murine gammaherpesvirus 68 open
448 reading frame 24 is required for late gene expression after DNA replication. J Virol
449 81:6761–6764.

450 16. Gruffat H, Kadjouf F, Mariame B, Manet E. 2012. The Epstein-Barr Virus BcRF1 Gene
451 Product Is a TBP-Like Protein with an Essential Role in Late Gene Expression. J Virol
452 86:6023–6032.

453 17. Wyrwicz LS, Rychlewski L. 2007. Identification of Herpes TATT-binding protein. Antiviral
454 Res 75:167–172.

455 18. Perng Y-C, Campbell JA, Lenschow DJ, Yu D. 2014. Human cytomegalovirus pUL79 is an
456 elongation factor of RNA polymerase II for viral gene transcription. PLoS Pathog
457 10:e1004350.

458 19. Pan D, Han T, Tang S, Xu W, Bao Q, Sun Y, Xuan B, Qian Z. 2018. Murine Cytomegalovirus
459 Protein pM91 Interacts with pM79 and Is Critical for Viral Late Gene Expression. J Virol

460 JVI.00675-18.

461 20. El-Guindy A, Lopez-Giraldez F, Delecluse HJ, McKenzie J, Miller G. 2014. A Locus
462 Encompassing the Epstein-Barr Virus bglf4 Kinase Regulates Expression of Genes
463 Encoding Viral Structural Proteins. PLoS Pathog 10:e1004307.

464 21. McKenzie J, Lopez-Giraldez F, Delecluse HJ, Walsh A, El-Guindy A. 2016. The Epstein-Barr
465 Virus Immunoevasins BCRF1 and BPLF1 Are Expressed by a Mechanism Independent of
466 the Canonical Late Pre-initiation Complex. PLoS Pathog 12:1–32.

467 22. Edgar RC. 2004. MUSCLE: Multiple sequence alignment with high accuracy and high
468 throughput. Nucleic Acids Res 32:1792–1797.

469 23. Brulois KF, Chang H, Lee a. S-Y, Ensser a., Wong L-Y, Toth Z, Lee SH, Lee H-R, Myoung J,
470 Ganem D, Oh T-K, Kim JF, Gao S-J, Jung JU. 2012. Construction and Manipulation of a
471 New Kaposi's Sarcoma-Associated Herpesvirus Bacterial Artificial Chromosome Clone. J
472 Virol 86:9708–9720.

473 24. Dill KA. 1985. Theory for the Folding and Stability of Globular Proteins. Biochemistry
474 24:1501–1509.

475 25. White SH. 1992. Amino acid preferences of small proteins. J Mol Biol 227:991–995.

476 26. Dixit PD, Maslov S. 2013. Evolutionary Capacitance and Control of Protein Stability in
477 Protein-Protein Interaction Networks. PLoS Comput Biol 9 (4): e1003023.

478 27. Avey D, Tepper S, Pifer B, Bahga A, Williams H, Gillen J, Li W, Ogden S. 2016. Discovery of
479 a Coregulatory Interaction between Kaposi ' s Sarcoma- Associated Herpesvirus ORF45
480 and the Viral Protein Kinase ORF36. J Virol 90:5953–5964.

481 28. Djavadian R, Chiu YF, Johannsen E. 2016. An Epstein-Barr Virus-Encoded Protein Complex

482 Requires an Origin of Lytic Replication In Cis to Mediate Late Gene Transcription. PLoS
483 Pathog 12:1–25.
484 29. Labo N, Miley W, Marshall V, Gillette W, Esposito D, Bess M, Turano A, Uldrick T,
485 Polizzotto MN, Wyvill KM, Bagni R, Yarchoan R, Whitby D. 2014. Heterogeneity and
486 Breadth of Host Antibody Response to KSHV Infection Demonstrated by Systematic
487 Analysis of the KSHV Proteome. PLoS Pathog 10(3): e1004046.
488 30. Gardner MR, Glaunsinger BA. 2018. Kaposi's Sarcoma-Associated Herpesvirus ORF68 is a
489 DNA Binding Protein Required for Viral Genome Cleavage and Packaging. J Virol
490 92:e00840-18.
491
492 **Figure 1**
493 ORF18 interacts with ORFs 30, 31, 34, and 66. (A) Diagram of vTA interactions in KSHV from (9).
494 (B-E) HEK293T cells were transfected with the indicated vTA plasmids, then subjected to co-IP
495 using α-FLAG beads followed by western blot analysis with the indicated antibody to detect
496 ORF18 and either ORF30 (*B*), ORF31 (*C*), ORF66 (*D*), and ORF34 (*E*). Input represents 2.5% of the
497 lysate used for co-IP. Vinculin served as a loading control. (F) HEK293T cells were transfected
498 with the indicated vTA plasmids. 24 h post transfection, cycloheximide was added to a final
499 concentration of 100 μg/ml, and samples were collected at the indicated time points after the
500 addition of cycloheximide. 25 μg of whole cell lysate was resolved using SDS-PAGE followed by
501 western blot with the indicated antibodies. Vinculin served as a loading control.
502
503

504 **Figure 2**

505 ORF18 mutant screen for interactions with ORFs 30, 31, and 66. (A) Diagram depicting the
506 conserved residues in KSHV ORF18 in a MUSCLE alignment with MHV68 ORF18, EBV BVLF1,
507 HCMV pUL79, MCMV pUL79, and BHV4 ORF18. Red color denotes amino acids found to have
508 interactions <10% of WT with any of the vTAs. (B) Heat map of the co-IP efficiency of each
509 ORF18 mutant against ORFs 30, 31, and 66.

510

511 **Figure 3**

512 Six ORF18 mutants are consistently defective for interaction with ORF30. (A-D) HEK293T cells
513 were transfected with the indicated vTA plasmids, then subjected to co-IP using α-FLAG beads
514 followed by western blot analysis to detect the ability of WT or mutant ORF18 to interact with
515 ORF30 (*A*), ORF31 (*B*), ORF34 (*C*), and ORF66 (*D*). The co-IP efficiency was calculated as
516 described in the text for 3-4 independent experimental replicates and plotted as bar graphs. In
517 *(A)*, the dotted line represents Y = 0.1, and in *(B-D)*, the dotted line represents Y = 1.0.

518

519 **Figure 4**

520 Impairing the interaction between ORF18 and ORF30 reduces activation of the late K8.1
521 promoter. (A) Diagram depicting the vector combinations that were transfected for the late
522 gene reporter assay. (B) HEK293T cells were transfected with the vTA plasmids including WT or
523 mutant ORF18, the K8.1 or ORF57 promoter reporter plasmids, and the pRL-TK Renilla plasmid
524 as a transfection control. 24 h post-transfection the lysates were harvested and luciferase

525 activity was measured. Data shown are from 3 independent biological replicates, with statistics
526 calculated using an unpaired t-test where (*) $p < 0.05$, (**) $p < 0.005$, and (***) $p < 0.0007$.
527
528 **Figure 5**
529 Disrupting the interaction between ORF18 and ORF30 weakens the assembly of the vTA
530 complex. HEK293T cells were transfected with the indicated vTA plasmids then subjected to co-
531 IP using α-FLAG beads followed by western blot analysis with the indicated antibody. Far right
532 boxed lane is a longer exposure of the $ORF18^{E36A_L37A}$ IP lane. Input represents 2.5% of the
533 lysate used for co-IP. Vinculin was used as a loading control.
534
535 **Figure 6**
536 Characterizing the effect of the E36A_L37A ORF18 mutation on the virus. (A) iSLK cells latently
537 infected with WT KSHV, 18.Stop KSHV, or 18.Stop complemented with $ORF18^{WT}$ or
538 $ORF18^{E36A_L37A}$ were induced to enter the lytic cycle with 1 μg/ml doxycycline and 1 mM sodium
539 butyrate. 72 h post induction, DNA was isolated and fold viral DNA replication was measured by
540 qPCR before and after induction of the lytic cycle. Data shown are from 5 independent
541 biological replicates. (B) Western blots of the expression of the early protein ORF59, the late
542 protein K8.1, $ORF18^{WT}$, and $ORF18^{E36A_L37A}$ in the indicated cell lines induced as described in (*A*).
543 GAPDH was used as a loading control. (C) HEK293T target cells were spinfected with filtered
544 supernatant from induced cells. Progeny virion production was measured 24 h after
545 supernatant transfer by flow cytometry of GFP+ target cells. Data shown are from 3

546 independent biological replicates with statistics calculated using an unpaired t-test where
547 (****) $p < 0.0001$.
548
549 **Figure 7**
550 Mutating E48_L49 in pUL79 disrupts its interaction with pUL91. (A) MUSCLE multiple sequence
551 alignment for HCMV pUL79 and homologs showing the location of conserved amino acids that
552 correspond to E36_L37 in KSHV ORF18. (B) HEK293T cells were transfected with the indicated
553 plasmids, then subjected to co-IP using α-FLAG beads followed by western blot analysis with
554 the indicated antibody. To normalize for the difference in expression of pUL91 in the different
555 transfection conditions, the co-IP efficiency was multiplied by the fold expression of pUL91 in
556 the presence of WT pUL79 versus E48A_L49A pUL79. Input represents 2.5% of lysate used for
557 co-IP. Vinculin was used as a loading control.
558
559
560
561
562
563
564
565
566
567
568
569
570
571
572
573
574
575
576
577

578 Table 1. Primer sequences used in this study

579

Primer Number	Purpose	Sequence 5' - 3'	Orientation
1	ORF18 (L29A)	CATGTGGCGCTTTTTGCAAAATAAGAATGCAAATACATTCCACGCCCAAG	F
2	ORF18 (L29A)	CTTGGGCGTGGAATGTATTTGCATTCTTATTTTGCAAAAAGCGCCACATG	R
3	ORF18 (E36A)	AATACATTCCACGCCCAAGCGCTGCGTTTTATTCATTTG	F
4	ORF18 (E36A)	CAAATGAATAAAACGCAGCGCTTGGGCGTGGAATGTATT	R
5	ORF18 (L37A)	GAACCAAATGAATAAAACGCGCCTCTTGGGCGTGGAATGTAT	F
6	ORF18 (L37A)	ATACATTCCACGCCCAAGAGGCGCGTTTTATTCATTTGGTTC	R
7	ORF18 (N63A)	GGGAGGCTACTGCCGCTGCCGGGACCTACG	F
8	ORF18 (N63A)	CGTAGGTCCCGGCAGCGGCAGTAGCCTCCC	R
9	ORF18 (G65A)	CTCGTCGTAGGTCGCGGCATTGGCAGT	F
10	ORF18 (G65A)	ACTGCCAATGCCGCGACCTACGACGAG	R
11	ORF18 (L72A)	GAACCTTGCGTCCCGCGACCACCTCGTCGT	F
12	ORF18 (L72A)	ACGACGAGGTGGTCGCGGGACGCAAGGTTC	R
13	ORF18 (R74A)	CGCAGGAACCTTGGCTCCCAGGACCACC	F
14	ORF18 (R74A)	GGTGGTCCTGGGAGCCAAGGTTCCTGCG	R
15	ORF18 (K75A)	GGTCCTGGGACGCGCGGTTCCTGCGGAG	F
16	ORF18 (K75A)	CTCCGCAGGAACCGCGCGTCCCAGGACC	R
17	ORF18 (W81A)	TCGTACACGAGCTTCGCCACCTCCGCAGGAAC	F
18	ORF18 (W81A)	GTTCCTGCGGAGGTGGCGAAGCTCGTGTACGA	R
19	ORF18 (Y85A)	TCCTCGAGCCCATCGGCCACGAGCTTCCACAC	F
20	ORF18 (Y85A)	GTGTGGAAGCTCGTGGCCGATGGGCTCGAGGA	R
21	ORF18 (L107A)	GTTCAAGTGCATCCAGGCGCTGTCCCGGTATGCC	F
22	ORF18 (L107A)	GGCATACCGGGACAGCGCCTGGATGCACTTGAAC	R
23	ORF18 (G130A)	GTCGTGGGTGACCGCTAGCCGGTGAAA	F
24	ORF18 (G130A)	TTTCACCGGCTAGCGGTCACCCACGAC	R
25	ORF18 (G145A)	CAGATTAAACAAAAAGTTTGCGTCCACCAGGTTTTCCG	F
26	ORF18 (G145A)	CGGAAAACCTGGTGGACGCAAACTTTTTGTTTAATCTG	R
27	ORF18 (N146A)	TTCCCAGATTAAACAAAAAGGCTCCGTCCACCAGGTTTTCCG	F
28	ORF18 (N146A)	CGGAAAACCTGGTGGACGGAGCCTTTTTGTTTAATCTGGGAA	R
29	ORF18 (L151A)	GAGCACACTTCCCGCATTAAACAAAAAGTTTCCGTCCACC	F
30	ORF18 (L151A)	GGTGGACGGAAACTTTTTGTTTAATGCGGGAAGTGTGCTC	R
31	ORF18 (G152A)	TGCAGGGGAGCACACTTGCCAGATTAAACAAAAAG	F
32	ORF18 (G152A)	CTTTTTGTTTAATCTGGCAAGTGTGCTCCCCTGCA	R
33	ORF18 (R158A)	CGCAAGGAGCAGCGCGCAGGGGAGCACA	F
34	ORF18 (R158A)	TGTGCTCCCCTGCGCGCTGCTCCTTGCG	R
35	ORF18 (L159A)	CGCCGCAAGGAGCGCCCTGCAGGGGAGC	F
36	ORF18 (L159A)	GCTCCCCTGCAGGGCGCTCCTTGCGGCG	R
37	ORF18 (W170A)	ATCGCTGCCCGCAAAGGCGAGGCAGTAGCCC	F

38	ORF18 (W170A)	GGGCTACTGCCTCGCCTTTGCGGGCAGCGAT	R
39	ORF18 (G171A)	CGTGTTCATCGCTGGCCCAAAAGGCGAGG	F
40	ORF18 (G171A)	CCTCGCCTTTTGGGCCAGCGATGAACACG	R
41	ORF18 (E176A)	GCGCACCCAGCGTGCGTGTTCATCGCT	F
42	ORF18 (E176A)	AGCGATGAACACGCACGCTGGGTGCGC	R
43	ORF18 (R180A)	CTGGGCGAAGAAGGCCACCCAGCGTTCG	F
44	ORF18 (R180A)	CGAACGCTGGGTGGCCTTCTTCGCCCAG	R
45	ORF18 (L191A)	AAGACGCCCGGAGACTATCGCGTAGCAAATGAAAAGCTTC	F
46	ORF18 (L191A)	GAAGCTTTTCATTTGCTACGCGATAGTCTCCGGGCGTCTT	R
47	ORF18 (G214A)	CCTCCACCGGAGCGGGATAGCCC	F
48	ORF18 (G214A)	GGGCTATCCCGCTCCGGTGGAGG	R
49	ORF18 (G228A)	GCATACGTTCGTATGGCGTACATGGAGCGGA	F
50	ORF18 (G228A)	TCCGCTCCATGTACGCCATACGAACGTATGC	R
51	ORF18 (E36A_L37A)	CAGAGAACCAAATGAATAAAACGCGCCGCTTGGGCGTGGAATGTATTTAAAT	F
52	ORF18 (E36A_L37A)	ATTTAAATACATTCCACGCCCAAGCGGCGCGTTTTATTCATTTGGTTCTCTG	R
53	ORF18 (R74A_K75A)	CCTCCGCAGGAACCGCGGCTCCCAGGACCACCTCGTC	F
54	ORF18 (R74A_K75A)	GACGAGGTGGTCCTGGGAGCCGCGGTTCCTGCGGAGG	R
55	ORF18 (G145A_N146A)	CTTCCCAGATTAAACAAAAAGGCTGCGTCCACCAGGTTTTCCGGGG	F
56	ORF18 (G145A_N146A)	CCCCGGAAAACCTGGTGGACGCAGCCTTTTTGTTTAATCTGGGAAG	R
57	ORF18 (L151A_G152A)	AGGGGAGCACACTTGCCGCATTAAACAAAAAGTTTCCGTCCACCA	F
58	ORF18 (L151A_G152A)	TGGTGGACGGAAACTTTTTGTTTAATGCGGCAAGTGTGCTCCCCT	R
59	ORF18 (R158A_L159A)	CCGCCGCAAGGAGCGCCGCGCAGGGGAGCACAC	F
60	ORF18 (R158A_L159A)	GTGTGCTCCCCTGCGCGGCGCTCCTTGCGGCGG	R
61	ORF18 (W170A_G171A)	GTGTTCATCGCTGGCCGCAAAGGCGAGGCAGTAGCC	F
62	ORF18 (W170A_G171A)	GGCTACTGCCTCGCCTTTGCGGCCAGCGATGAACAC	R
63	pLVX-TetOneZeo	TTTTTGGAGGCCTAGGCTTTTGCAAAACGCGACCATGGCCAAGTTGACCAGTGC	F
64	pLVX-TetOneZeo	ATTGTTCCAGACGCGTTCAGTCCTGCTCCTCGGC	R
65	2xStrep-ORF34 pCDNA4	GAGAAGGGGGCGGCCTTTGCTTTGAGCTCGCTCGTGT	F
66	2xStrep-ORF34 pCDNA4	AAACGGGCCCTCTAGTTAGAGTTGGTTGAGTCCATTCTCCTTGATC	R
67	UL79-3xFLAG pCDNA4	TACCGAGCTCGGATCATGATGGCCCGCGACG	F
68	UL79-3xFLAG pCDNA4	CTCCCTCGAGCGGCCCCACGTCGTTAGCCAGCGT	R
69	UL91-2xStrep pCDNA4	TACCGAGCTCGGATCATGAACTCGTTGCTGGCGG	F
70	UL91-2xStrep pCDNA4	CTCCCTCGAGCGGCCCTGTCACAGGCGCCCGAG	R
71	ORF18^{WT} and ORF18^{E36_L37A} pLVX TetOneZeo	CCCTCGTAAAGAATTATGCTCGGAAAATACGTGTGTGAGACC	F
72	ORF18^{WT} and ORF18^{E36_L37A} pLVX TetOneZeo	GAGGTGGTCTGGATCTTAAACGGGCCCCTTGTCGTCG	R
73	UL79^{E48_L49A}-3xFLAG pCDNA4	ATGAGGCGTACGATCTTGGCTGCTTCCAAACGCAGCGAGC	F
74	UL79^{E48_L49A}-3xFLAG pCDNA4	GCTCGCTGCGTTTGGAAGCAGCCAAGATCGTACGCCTCAT	R
75	ORF59 promoter qPCR	AATCCACAGGCATGATTGC	F
76	ORF59 promoter qPCR	CACACTTCCACCTCCCCTAA	R

77	GAPDH promoter qPCR	TACTAGCGGTTTTACGGGCG	F
78	GAPDH promoter qPCR	TCGAACAGGAGGAGCAGAGACCGA	R

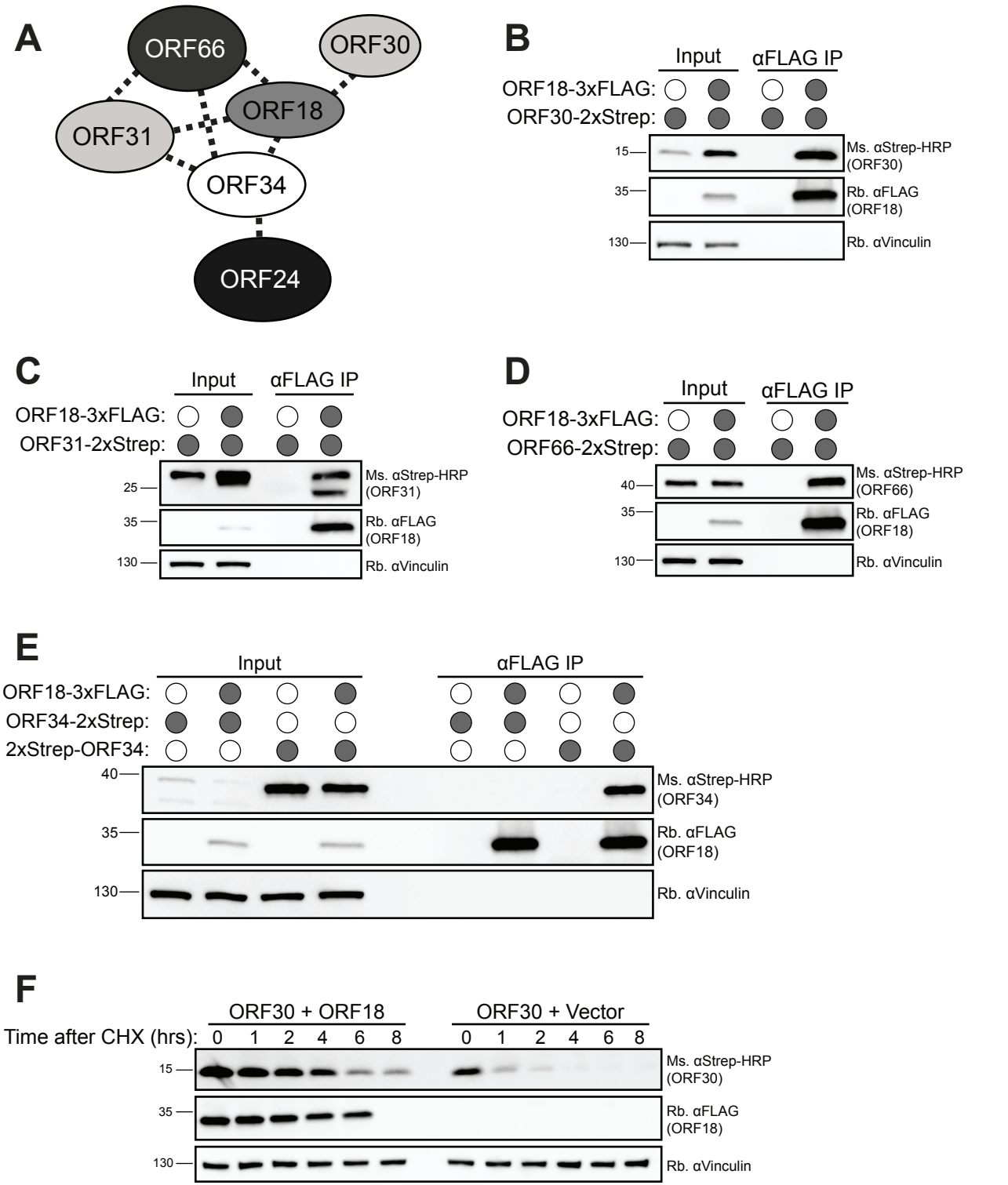
A
ORF66
ORF30
ORF18
ORF31
ORF34
ORF24
B
Input
αFLAG IP
ORF18-3xFLAG:
ORF30-2xStrep:
15
35
130
Ms. αStrep-HRP (ORF30)
Rb. αFLAG (ORF18)
Rb. αVinculin
C
Input
αFLAG IP
ORF18-3xFLAG:
ORF31-2xStrep:
25
35
130
Ms. αStrep-HRP (ORF31)
Rb. αFLAG (ORF18)
Rb. αVinculin
D
Input
αFLAG IP
ORF18-3xFLAG:
ORF66-2xStrep:
40
35
130
Ms. αStrep-HRP (ORF66)
Rb. αFLAG (ORF18)
Rb. αVinculin
E
Input
αFLAG IP
ORF18-3xFLAG:
ORF34-2xStrep:
2xStrep-ORF34:
40
35
130
Ms. αStrep-HRP (ORF34)
Rb. αFLAG (ORF18)
Rb. αVinculin
F
ORF30 + ORF18
ORF30 + Vector
Time after CHX (hrs): 0 1 2 4 6 8 0 1 2 4 6 8
15
35
130
Ms. αStrep-HRP (ORF30)
Rb. αFLAG (ORF18)
Rb. αVinculin

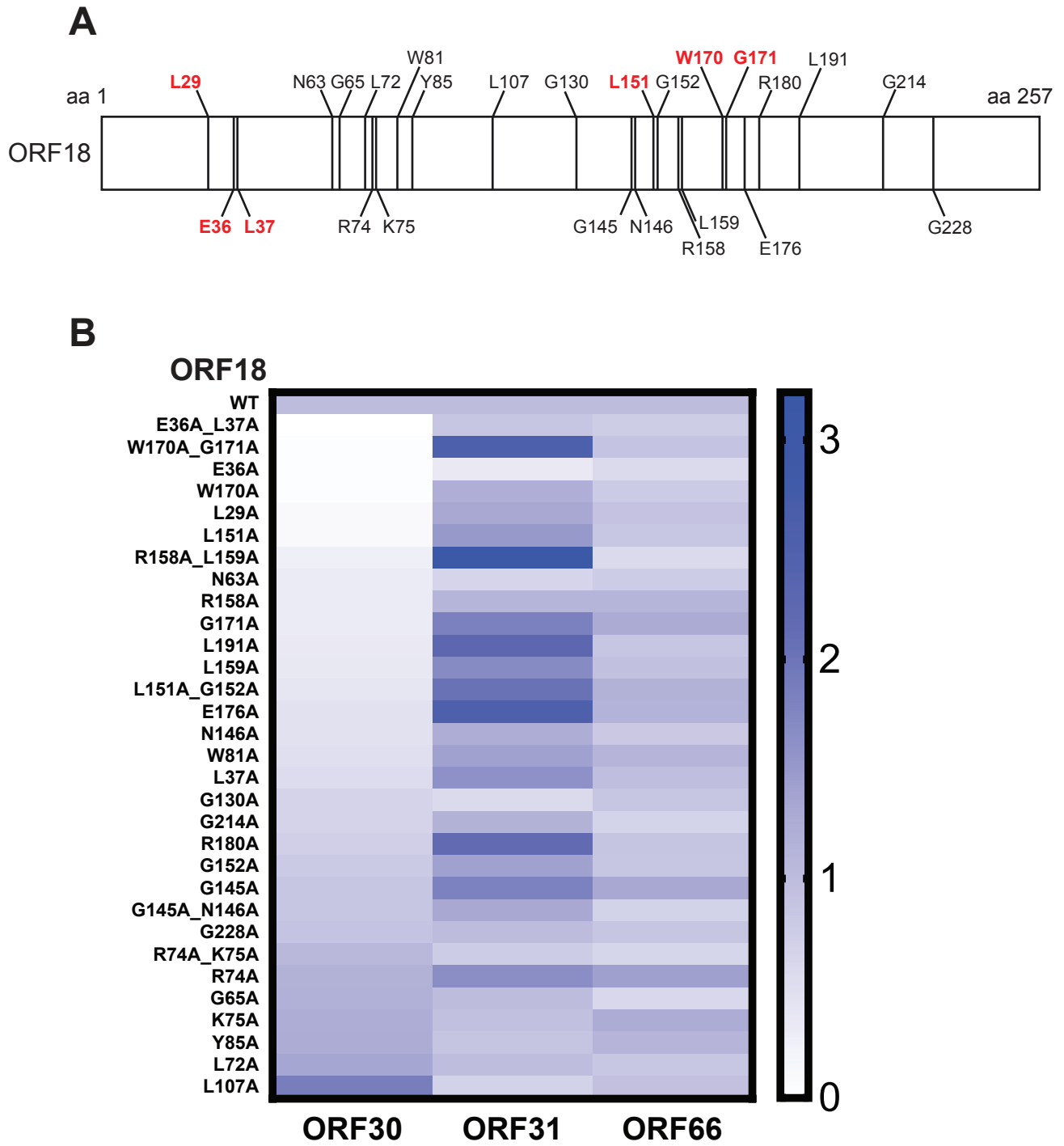
A
aa 1
aa 257
ORF18
L29
N63
G65
L72
W81
Y85
L107
G130
L151
G152
W170
G171
L191
R180
G214
E36
L37
R74
K75
G145
N146
L159
R158
E176
G228
B
ORF18
WT
E36A_L37A
W170A_G171A
E36A
W170A
L29A
L151A
R158A_L159A
N63A
R158A
G171A
L191A
L159A
L151A_G152A
E176A
N146A
W81A
L37A
G130A
G214A
R180A
G152A
G145A
G145A_N146A
G228A
R74A_K75A
R74A
G65A
K75A
Y85A
L72A
L107A
ORF30
ORF31
ORF66
3
2
1
0

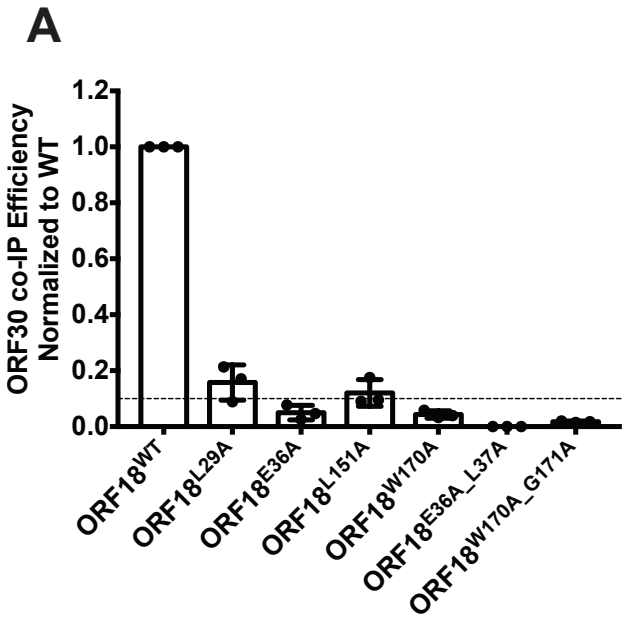
A
ORF30 co-IP Efficiency
Normalized to WT
1.2
1.0
0.8
0.6
0.4
0.2
0.0
ORF18WT
ORF18L29A
ORF18E36A
ORF18L151A
ORF18W170A
ORF18E36A_L37A
ORF18W170A_G171A

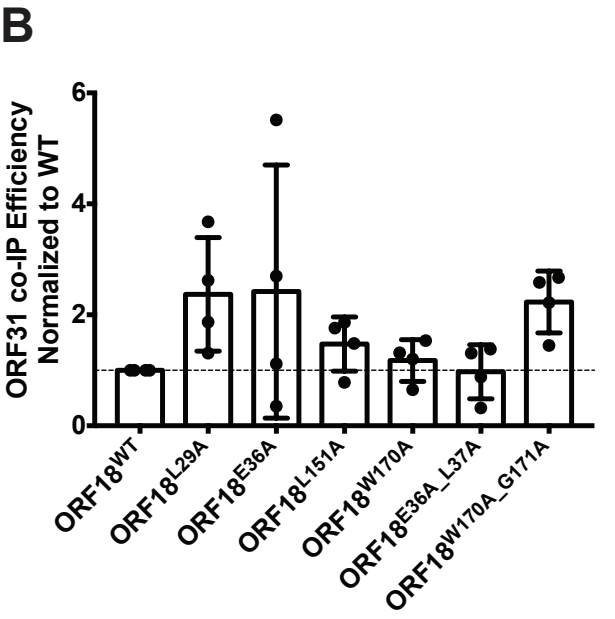
B
ORF31 co-IP Efficiency
Normalized to WT
6
4
2
0
ORF18WT
ORF18L29A
ORF18E36A
ORF18L151A
ORF18W170A
ORF18E36A_L37A
ORF18W170A_G171A

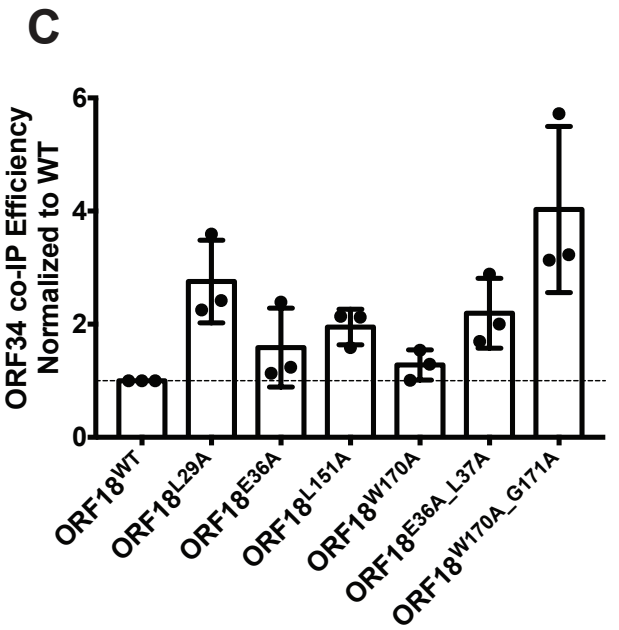
C
ORF34 co-IP Efficiency
Normalized to WT
6
4
2
0
ORF18WT
ORF18L29A
ORF18E36A
ORF18L151A
ORF18W170A
ORF18E36A_L37A
ORF18W170A_G171A

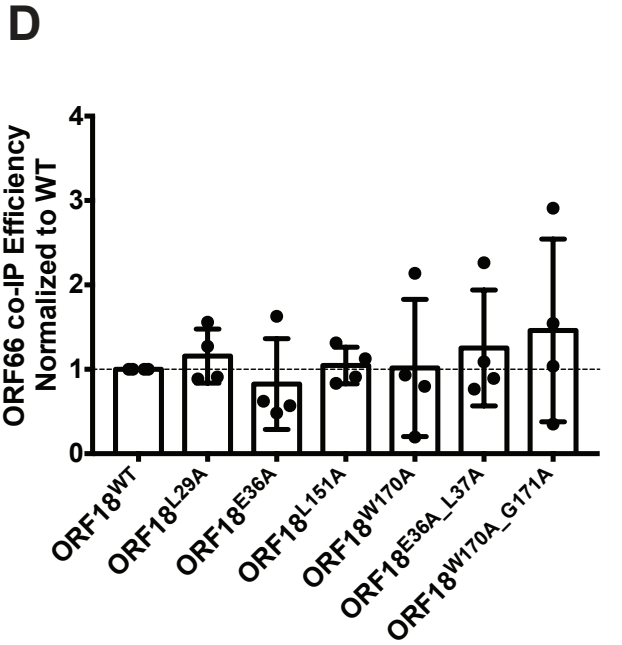
D
ORF66 co-IP Efficiency
Normalized to WT
4
3
2
1
0
ORF18WT
ORF18L29A
ORF18E36A
ORF18L151A
ORF18W170A
ORF18E36A_L37A
ORF18W170A_G171A

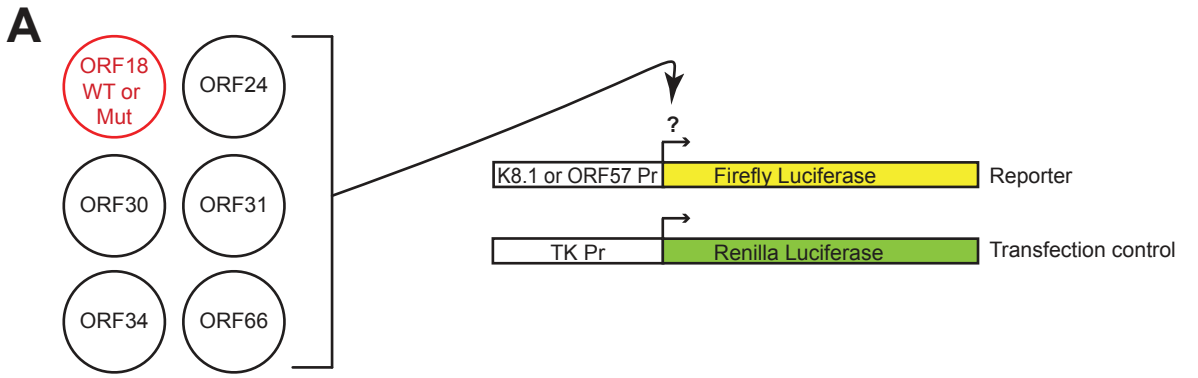
A
ORF18 WT or Mut
ORF24
ORF30
ORF31
ORF34
ORF66
?
K8.1 or ORF57 Pr
Firefly Luciferase
Reporter
TK Pr
Renilla Luciferase
Transfection control

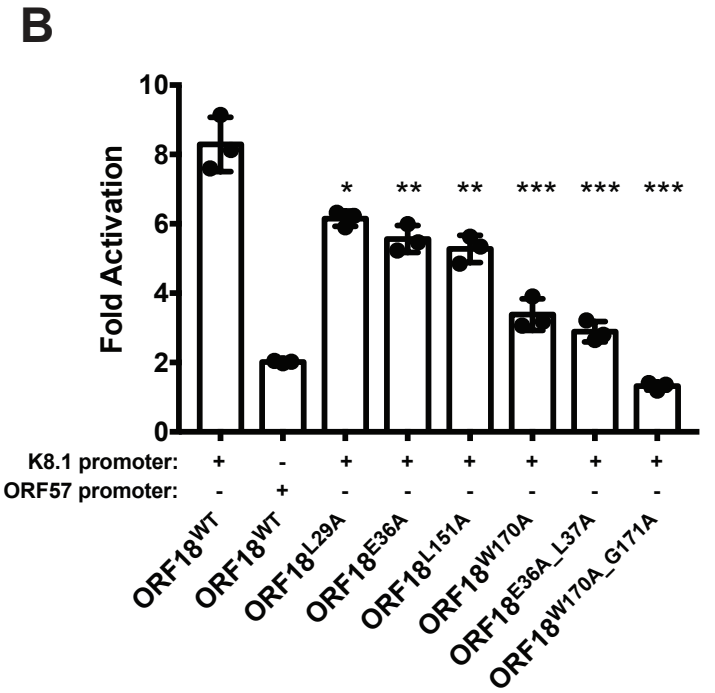
B
Fold Activation
10
8
6
4
2
0
*
**
**
***
***
***
K8.1 promoter: + - + + + + + +
ORF57 promoter: - + - - - - - -
ORF18WT
ORF18WT
ORF18L29A
ORF18E36A
ORF18L151A
ORF18W170A
ORF18E36A_L37A
ORF18W170A_G171A

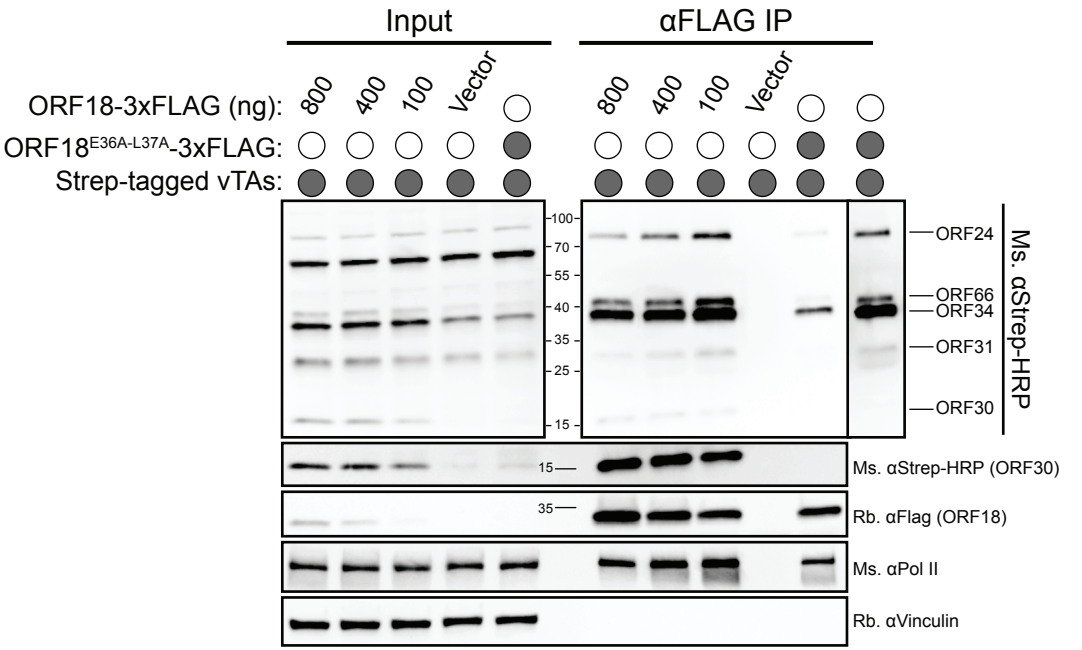
Input
αFLAG IP
ORF18-3xFLAG (ng):
800
400
100
Vector
800
400
100
Vector
ORF18E36A-L37A-3xFLAG:
Strep-tagged vTAs:
100
70
55
40
35
25
15
ORF24
ORF66
ORF34
ORF31
ORF30
Ms. αStrep-HRP
15
Ms. αStrep-HRP (ORF30)
35
Rb. αFlag (ORF18)
Ms. αPol II
Rb. αVinculin

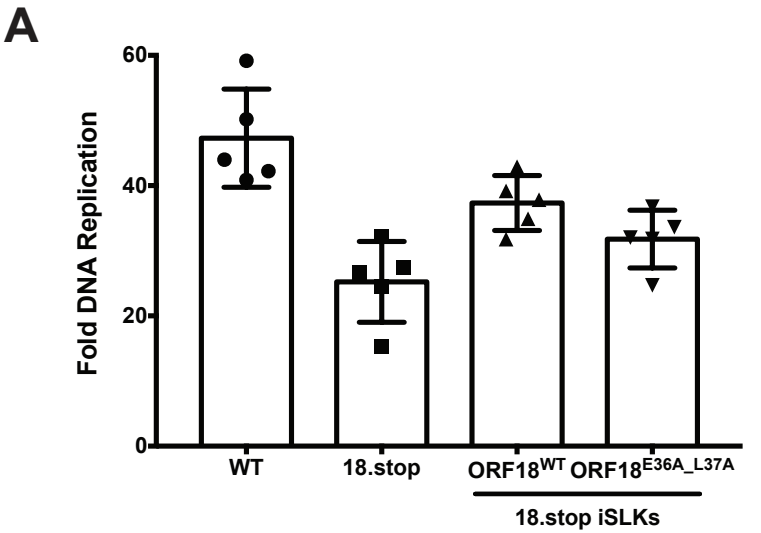
A
Fold DNA Replication
60
40
20
0
WT
18.stop
ORF18WT
ORF18E36A_L37A
18.stop iSLKs

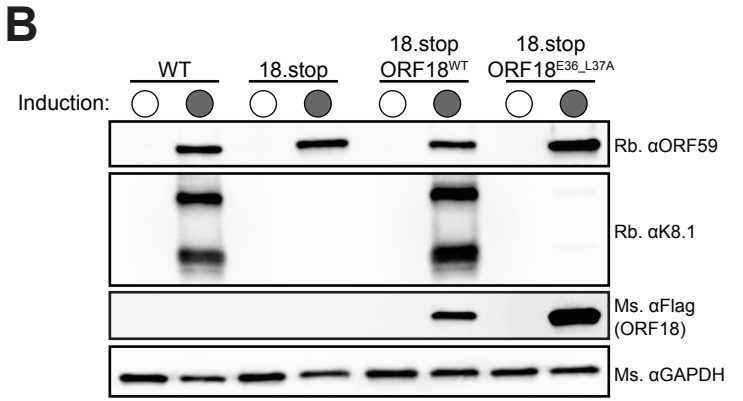
B
WT
18.stop
18.stop ORF18WT
18.stop ORF18E36_L37A
Induction:
Rb. αORF59
Rb. αK8.1
Ms. αFlag (ORF18)
Ms. αGAPDH

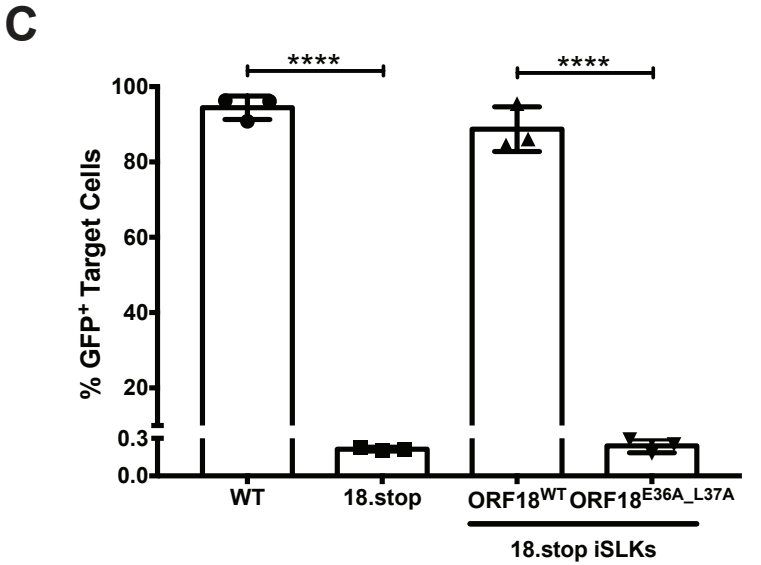
C
% GFP+ Target Cells
100
80
60
40
20
0.3
0.0
****
****
WT
18.stop
ORF18WT
ORF18E36A_L37A
18.stop iSLKs

A

HCMV pUL79	$_{40}$LSSLRLE**EL**KIVRLIC$_{57}$
MCMV pM79	$_{32}$LSSMRLE**EL**KIIRLAC$_{49}$
EBV BVLF1	$_{50}$LCALRED**EL**RFLHLSL$_{67}$
KSHV ORF18	$_{28}$LNTFHAQ**EL**RFIHLVL$_{44}$
MHV68 ORF18	$_{41}$LNTLSST**EL**RLLHAIL$_{58}$
BHV ORF18	$_{28}$LNTYTDE**EL**KFTHMVL$_{44}$
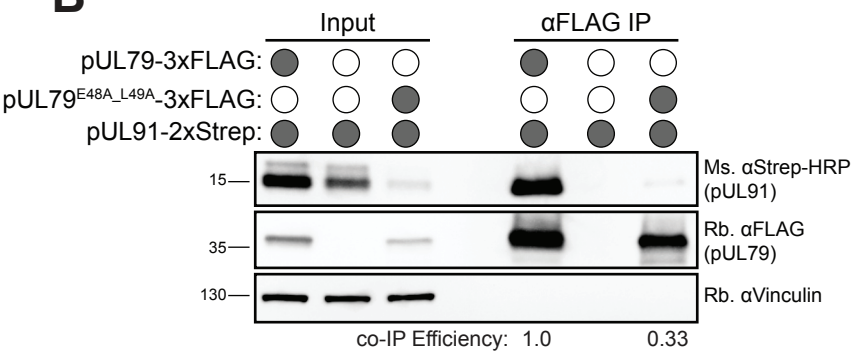
B